

Uncertainty Analysis of SEBS Daily Evapotranspiration Estimation Input Parameters (SEBS)

¹Mohamed Elhag and ²Haneen Alsubaie

¹Department of Hydrology and Water Resources Management, Faculty of Meteorology,
Environment & Arid Land Agriculture, King Abdulaziz University, Jeddah, 21589, Saudi Arabia

²Biological Sciences Department, Faculty of Science, King Abdulaziz University, Jeddah 21589, Saudi Arabia

Abstract: Assessment of evapotranspiration is always a foremost element in water resources management. The consistent assessment of daily evapotranspiration provisions decision makers to review the existing land use practices in terms of water management, while empowering them to recommend accurate land use changes. Earth observation satellite sensors are used in conjunction with Surface Energy Balance (SEB) models to overcome difficulties in obtaining daily evapotranspiration quantities on a regional scale. SEB System (SEBS) is used to estimate daily evapotranspiration and an evaporative fraction over the Nile Delta along with data acquired by the Advance Along Track Scanning Radiometer (AATSR) and 15 in situ meteorological stations. The consequential maps and the following correlation analysis show resilient agreement, signifying SEBS' applicability and accurateness in the estimation of daily evapotranspiration over agricultural areas. Sensitivity analysis evaluates the influences of the inputs to the total uncertainty in the analysis outcomes. SEBS inputs parameters are interconnected. Interconnections between different metrological features are anticipated, but the magnitude of the features sensitivity is uncertain. Seven different metrological features are involved in providing a comparative analysis of Gaussian process emulators for performing a global sensitivity analysis (GSA). Conclusions conducted from the current work are anticipated to contribute decisively towards an inclusive SEBS inputs parameter assessment of its overall verification.

Key words: Global sensitivity analysis • Metrological data • SEBS • Uncertainty

INTRODUCTION

The key for efficient water resources management for a regional scale is the estimation of accurate and reliable water requirements for irrigation purposes. Evapotranspiration is the major consumptive use of irrigation water in agriculture. Any attempt to improve the efficiency of the water supply system should be based on reliable estimates of daily evapotranspiration, which includes water evaporation from land and water surfaces and transpiration by vegetation [1]. Daily evapotranspiration is recognized as an essential process in determining the surface and mass energy interaction for any water resources management related to agriculture practices [2].

Daily evapotranspiration varies regionally and seasonally according to weather and wind conditions [3].

Understanding these variations in evapotranspiration is essential for managers responsible for planning and management of water resources, especially in arid and semi-arid regions [4]. At a field scale, actual daily evapotranspiration can be measured over a homogenous surface using conventional techniques, such as the Bowen Ratio (BR), Eddy Covariance (EC) and lysimeter systems. However, these systems do not provide spatial coverage indicated at the regional scale, especially in regions with advective climatic conditions.

Remote sensing is identified as an important tool supporting the management of natural resources and agricultural practices for wider spatial coverage. Thus remote sensing based daily evapotranspiration models better suit the estimation of crop water use at a regional agriculture scale [1,5,6].

Corresponding Author: Mohamed Elhag, Department of Hydrology and Water Resources Management, Faculty of Meteorology, Environment & Arid Land Agriculture, King Abdulaziz University, Jeddah, 21589, Saudi Arabia.
E-mail: melhag@kau.edu.sa.

The algorithms for the estimation of daily evapotranspiration using remote sensing data are basically calculating the sensible heat flux in order to obtain the latent heat flux [7,8,9]. However, the implementation of the algorithms remains valid in small-scale regions as it fails on the large scale due to surface geometry and thermal variability as well as lack of meteorological consistency [10,11,12,13,14,15].

One of the recent and most adequate algorithms for daily evapotranspiration estimation for agriculture lands is the Surface Energy Balance System (SEBS) developed by Su, [16,17]. SEBS takes into account different land surface physical and biological parameters that are derived from both AATSR and MERIS imagery. These parameters are best suited as input parameters in the SEBS model for reliable results in comparison with other relevant models [15,18].

Global sensitivity analysis (GSA) methods assign the output inconsistency to the inconsistency of the input parameters when they vary over their whole uncertainty domain [19]. The sensitivity of the input parameters is basically examined based on the generation of samples distributed across the parameter domain of interest. A comprehensive review of the available GSA methods and their applications is provided, for example, by Saltelli *et al.* [20,21], Saltelli [22]. GSA is a powerful tool due to its ability to integrate the influence of the input parameters over their whole range of discrepancy [23]. GSA techniques are able to deliver quantitative estimates not only of the most sensitive model inputs but also of the model input parameter interactions [24], yielding quantitative information on the degree of complexity of the model input–output interactions [19].

The aim of uncertainty analysis was to determine how sensitive the output of remotely sensed ET is, which are subject to uncertainty or variability. This is useful as a guiding tool when the model is under development as well as to understand model behavior when it is used for prediction or for decision support.

MATERIALS AND METHODS

Study Area: The Nile Delta was selected for this study because it is representative of farming scenarios in the whole Egypt (different agricultural systems, different soil types, different systems of fertilizer application, irrigation and drainage systems); consequently, the research in this study area can be applied to farms in other regions of Egypt. Also, the problems affecting agriculture in this area are a miniature of that of the entire territory (salinity, alkalinity and water logging). The huge triangle of the Nile Delta extends to the north of Cairo between Lake Mareotis in the west and the Suez Canal in the east, forming a wide arc along the Mediterranean coast bordered by lagoons and sand spits. Formed over millions of years by the deposits of mud brought down by the regular annual inundation and sediment transport and deposition of Nile, it marks the end of the river's long journey; when emerging from its narrow bed at the edge of the desert plateau, it breaks up into separate arms which pursue their meandering courses toward the sea [25]. This study was carried out in one of the main agricultural regions of Egypt represented by several Governorates located centrally at 30.07°N, 30.57°E. The Governorates are as follows: Alexandria, Buhayra, Cairo, Daqahliya, Damietta, Gharbiya, Ismailia, Kafr El-Sheikh, Minufiya, Port Said, Qalyubiya, Sharqiya and Suez and cover around 25,000 km² in total representing 2.5 % of the total area of Egypt (Figure 1). The most significant factors of land degradation are as follows: (a) wind, (b) water erosion, (c) water logging, (d) salinization and (e) soil compaction. On the other hand, land reclamation processes, enclosing the wider Delta region, are very pronounced due to human activities. The land use and land cover categories are as follows: (a) agriculture, (b) bare soil, (c) sand area, (d) salt flat, (e) swamps, (f) salt, (g) fish farms, (h) water bodies, and (i) urban areas [26].

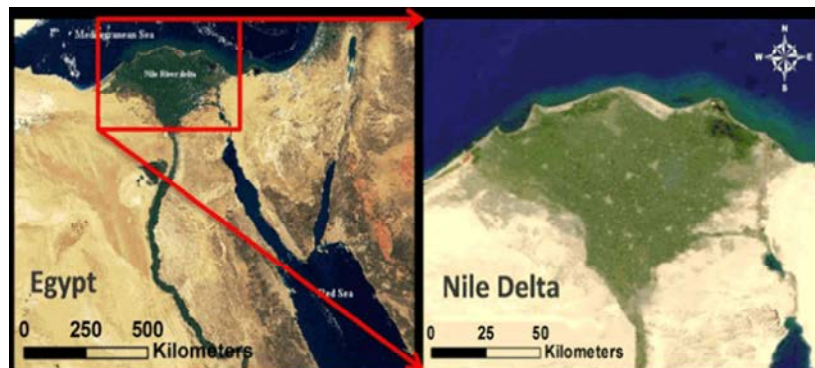


Fig. 1: Location map of the study area [27].

Data Sets: The application of the SEBS algorithm requires parameters derived from three different data sets: 1) AATSR data, 2) MERIS data and 3) Meteorological data. These data sets are described in the following subheadings.

AATSR: The AATSR sensor has a spatial resolution of 1 km at nadir. AATSR has three channels at thermal infrared wavelengths, from which surface temperatures are derived over both sea and land surfaces. In addition, AATSR has four visible and near-infrared wavelength channels, which are commonly used to identify cloudy areas and to measure solar radiation that is scattered and reflected from the Earth's surface and atmosphere [28]. The principal objective of the sensor is to provide data with high levels of accuracy and revisiting frequency required for monitoring and carrying out research regarding the Earth's climate. The image used was acquired on the 10th of August 2007.

MERIS: The MERIS sensor has a spatial resolution of 1 km at nadir designed to acquire data over the Earth whenever illumination conditions are suitable [28]. The primary objective of MERIS is to derive estimates of the concentration of chlorophyll-a and suspended sediments in the water. MERIS is very useful to monitor the evolution of terrestrial environments, such as the fraction of the solar radiation effectively used by plants in the process of photosynthesis. The image used was acquired on the 9th of August 2007.

Meteorological Data: Six different weather stations located in the study area were used to obtain the average meteorological input data for the purpose of this study. The meteorological data used are: a) mean temperature, measured using a psychrometer, b) wind speed, measured using the CSAT3 instrument by Campbell, c) humidity, measured using hygrometers, d) surface pressure, measured using the PTB101b instrument and e) solar radiation, measured using the CNR1 instrument by Kipp and Zonen. The data were collected during August 2007.

SEBS Model: The model consists of a) a set of tools for the determination of the physical and biological parameters of the surface, such as albedo, emissivity, temperature and vegetation coverage, b) a model for the determination of the roughness length for heat transfer and c) a formulation for the determination of the evaporative fraction on the basis of energy balance at limiting meteorological conditions [16,17,18]. Following Su [17], the SEBS basic equations are:

$$R_n = G_0 + H + \lambda \times E \quad (1)$$

Where

R_n net radiation measured in watt per square meter,
 G_0 soil heat flux measured in watt per square meter,
 H turbulent sensible heat flux measured in watt per square meter,
 λE turbulent latent heat flux measured in watt per square meter,
 λ latent heat of vaporization measured in watt per square meter and
 E actual evaporation measured in millimeters per day.

H is the actually sensible heat flux and determined by the bulk atmospheric similarity approach. The actually sensible heat flux is limited by the H_{dry} and H_{wet} limiting conditions. H_{dry} and H_{wet} are derived by a combination equation following Menenti [29] holding the assumption of having a complete wet condition [30,31]. Therefore the daily evapotranspiration E_{daily} is expressed as:

$$E_{daily} = \Lambda_0^{24} \times 8.64 \times 10^7 \times \frac{R_n - G_0}{\lambda \rho \omega} \quad (2)$$

Where

Λ_0^{24} daily evaporative fraction,
 \bar{n}_a density of water measured in kilograms per cubic meter.

Validation: A total number of 120 points uniformly distributed over the study area to collect daily evapotranspiration values using lysimeter method according to Liu and Wang [32] with calibrated accuracy set to ± 0.025 . The collection of actual daily evapotranspiration points were done in the proximity of 1 km² of the selected points due to accessibility limitations and to stay within the one-pixel size of the AATSR sensor. The simulated daily evapotranspiration values conducted from SEBS were tested against the actual daily evapotranspiration values conducted from Lysimeter method.

Global Sensitivity Analysis Concept: Consistent with Saltelli *et al.* [20], GSA is the study of the relations between the input and the output of a model. Basically, sensitivity analysis is dealing with the variation correspondingly the uncertainties of the input magnitudes. Moreover, input parameters introduced to uncertainties of the model parameters and to the overall model structure. The discrepancy of the input parameters encounters discrepancies of the output magnitudes.

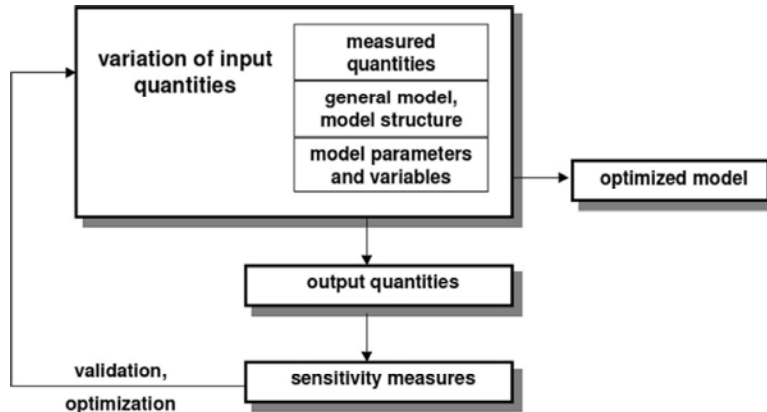


Fig. 2: General procedure for sensitivity analysis [24]

The interconnections between speckled input and output are measured by different sensitivity measures that are the basis for model validation and optimization [24]. The broad practice of sensitivity analysis is shown in Figure 2. GSA is an emphasis on variance-based techniques to estimate global, quantitative and model independent sensitivity measures.

Based on Monte Carlo methods, sensitivity analysis is methods are regression and correlation analysis as well as analysis of rank-transformed data. The general procedure to estimate global sensitivity measures is founded on the following equations:

$$S_i = \frac{\sigma_{E(Y/X_i)}^2}{\sigma_Y^2} \quad (3)$$

Where

$\sigma_{E(Y/X_i)}^2$ is the conditional variance

σ_Y^2 is the unconditional variance

For non-correlated input additive models:

$$\sum_{i=1}^n S_i = 1 \quad (4)$$

According to Schwiager, [24], this leads to an easy quantitative interpretation of the sensitivity indices, because each S_i delivers a direct measure for the portion of X_i on the output variance σ_Y^2 . For non additive models the inter actions among the input quantities with in the model have to be taken in to account. Non-additive models need a complete decomposition of the function Y into summands of increasing order:

$$\begin{aligned} & \sum_{i=1}^n S_i + \sum_{i=1}^n \sum_{j=i+1}^n S_{i,j} \\ & + \sum_{i=1}^n \sum_{j=i+1}^n \sum_{k=j+1}^n S_{i,j,k} \\ & + \dots + \sum \dots \dots S_{i,j,k,\dots,n} = 1 \end{aligned} \quad (5)$$

The terms of higher order are estimated by holding more than one input quantity fixed:

$$S_{i,j} = \frac{\sigma_{E(Y/X_i,X_j)}^2}{\sigma_Y^2} - S_i - S_j \quad (6)$$

Estimation of higher order terms leads to the estimation of total effects S_{Ti} with respect to an input quantity X_i to be computed as follows:

$$\begin{aligned} S_{Ti} &= S_i + \sum_{i=1}^n S_i + \sum_{i=1}^n \sum_{j=i+1}^n S_{i,j} \\ & + \sum_{i=1}^n \sum_{j=i+1}^n \sum_{k=j+1}^n S_{i,j,k} \\ & + \dots + \sum \dots S_{i,j,k,\dots,n} \text{ mit } j, k \neq i, j \neq k \end{aligned} \quad (7)$$

Corresponding total effect is computed as following:

$$S_{Ti} = 1 - \frac{\sigma_{E(Y/X_{\sim i})}^2}{\sigma_Y^2} \quad (8)$$

Consistently, a judgment between S_i and S_{Ti} lead to a conclusion concerning the additivity of models with non-correlated input: $S_{Ti} = S_i$ for additive model and $S_{Ti} > S_i$ for the non-additive model.

RESULTS AND DISCUSSIONS

The spatial distribution of daily evapotranspiration values varies over the Nile Delta region: The maximum daily evapotranspiration values are located at the East and West side of the Delta, while in the middle region of

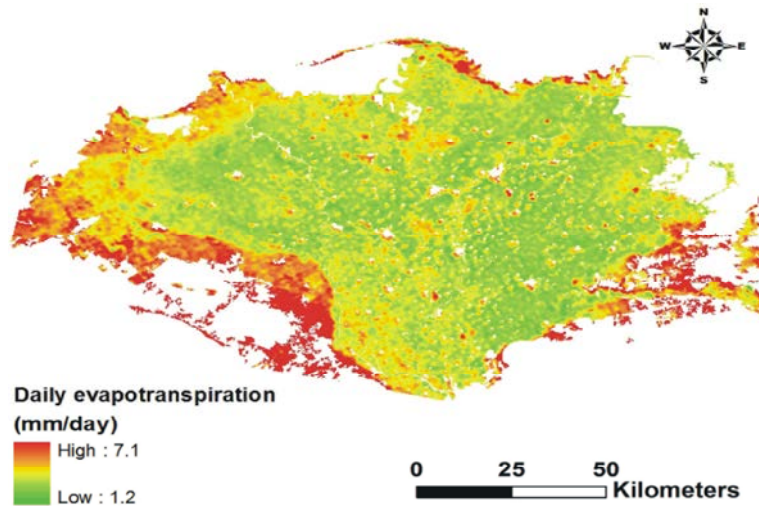


Fig. 3: SEBS daily evapotranspiration map

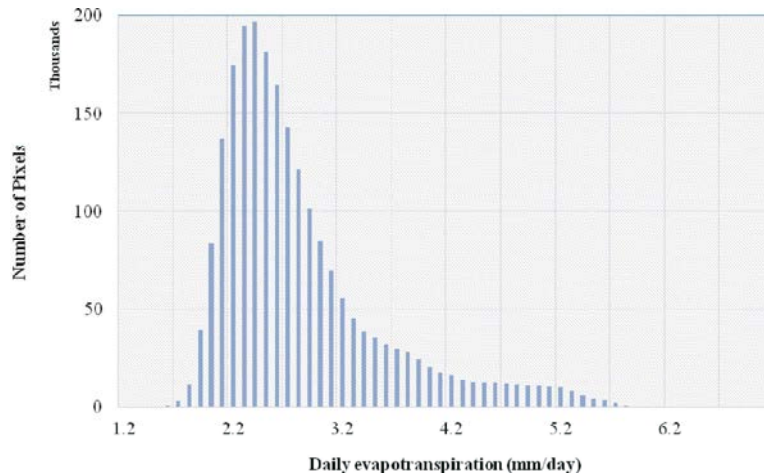


Fig. 4: Frequency distribution of simulated daily evapotranspiration values

the Delta, daily evapotranspiration values range from low to medium, which is also reported in Psilovikos and Elhag [33]; as illustrated in Figure 3.

The normal distribution of the daily evapotranspiration values is shown in Figure 4. Values less than 1.5 mm day⁻¹ and more than 6 mm day⁻¹ fall within a very small range of frequencies. The highest daily evapotranspiration values are concentrated around 2.5 mm d⁻¹ representing the majority of the Nile Delta agricultural area located centrally so that it may be recognized as “old land cultivation”. The new reclaimed agricultural land in the Nile Delta indicates a wider range of daily evapotranspiration values ranging from 4 mm d⁻¹ to 6 mm d⁻¹. The mean of the daily evapotranspiration values is 4.35 mm d⁻¹ and the standard deviation is 1.91 mm d⁻¹.

The high correlation coefficient indicates the reliability of using the linear equation in order to obtain

the daily evapotranspiration from satellite imagery [34,35]. This equation is of significant practical use, where information about water balance is needed to determine the irrigation requirements of various crops in various locations around the country or under similar conditions [36].

According to the regression equation explained in Figure 5 ($Y=0.9871x$ and $R^2=0.8412$), the application of the SEBS model over the Nile Delta region is highly correlated with the measurements of the ground truth data. The idea behind finding the best-fit line is based on the assumption that the data are actually scattered along a straight line called the least squares regression line, represented by the aforementioned equation [37,38].

The results of the sensitivity analysis are presented in Figures 6-12, focusing specifically on the decomposition of variance (%) of the mean total variance in emulator output, when input parameters have been

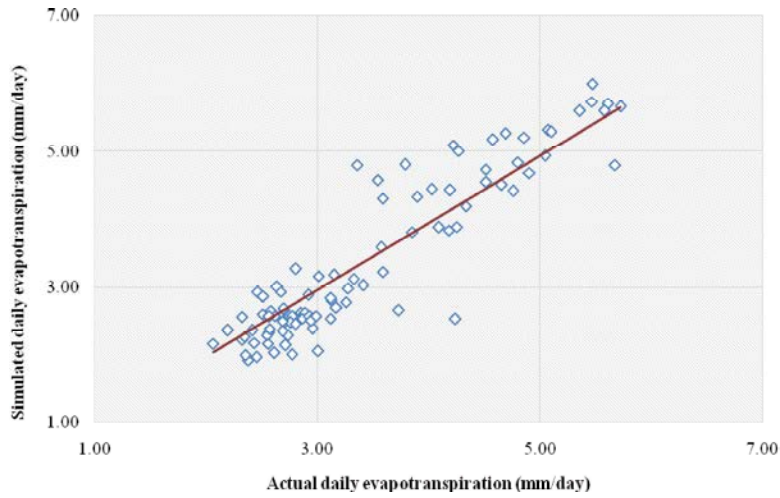


Fig. 5: Correlation between actual daily and simulated daily evapotranspiration

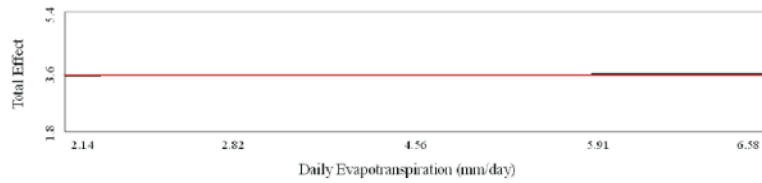


Fig. 6: Daily evapotranspiration uncertainty variances

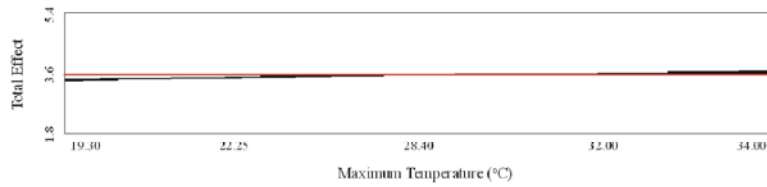


Fig. 7: Maximum temperature uncertainty variances

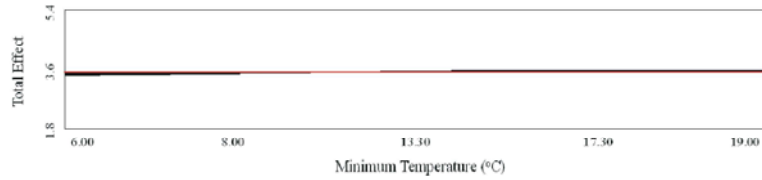


Fig. 8: Minimum temperature uncertainty variances

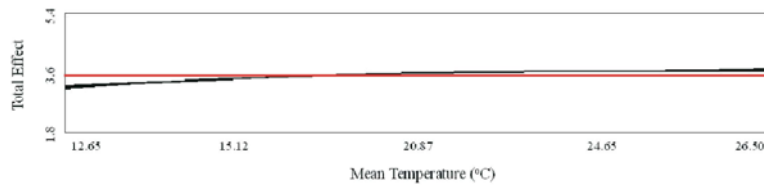


Fig. 9: Mean temperature uncertainty variances

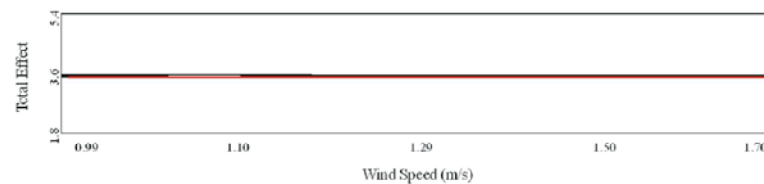


Fig. 10: Windspeed uncertainty variances

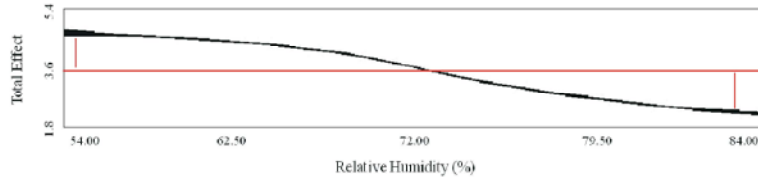


Fig. 11: Relative humidity uncertainty variances

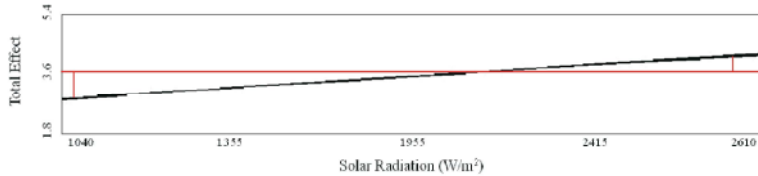


Fig. 12: Solar radiation uncertainty variances

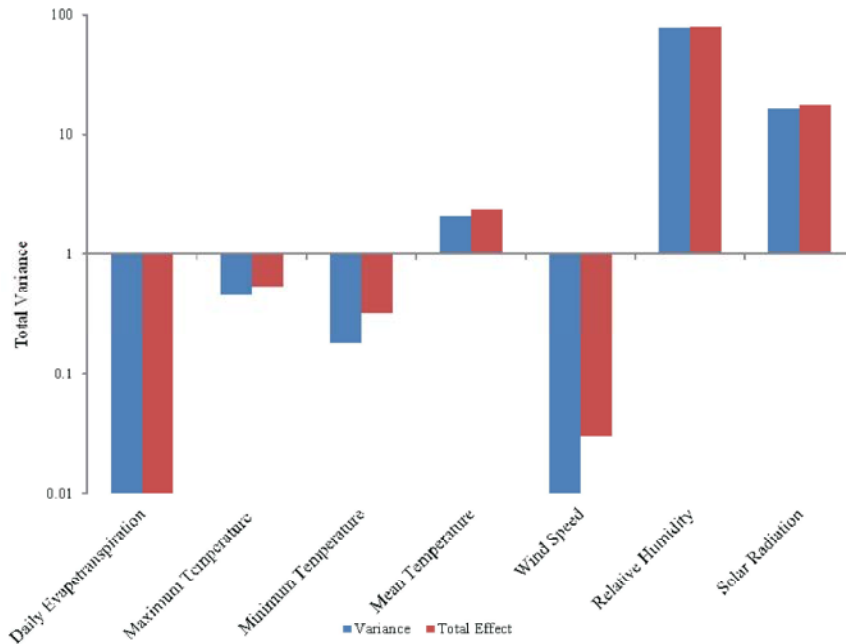


Fig. 13: Total variance of SEBS model input parameter

assumed non-correlated, normally distributed and varying within their whole range. Red lines in the following Figures represent the mean and the standard deviation from the mean total effects according to Saltelli, *et al.* [20]. The relative sensitivity of the model input parameters with respect to the sensitivity of the daily evapotranspiration estimated in the study area can be found in Table 1 and sensitivity total effect in chart representation (Figure 13).

Estimated daily evapotranspiration expressed the maximum certainty with total variances of 0.01. In Figures 7, 8 and 9, the different extent of temperatures demonstrated a relatively steady certainty variances. Meanwhile, the total of the effect of temperature increment

was accompanied by a slight deviation from the mean variances [39]. Wind speed (Figure 10) confirmed the exact behavior of daily evapotranspiration with total variances of 0.01. Higher and lower percentages of Relative humidity illustrated in Figure 11 suggested the highest uncertainty variances (79.04). The aforementioned uncertainty value draws the attention that the rule of relative humidity in daily evapotranspiration using SEBS model was not well defined yet due to total effect fluctuation behavior [19]. Solar radiation total effect is proportionally related to uncertainty variances (Figure 12). Furthermore, higher solar radiation values are closely related to the mean total variances rather than lower solar radiation values [40].

Table 1: SEBS input parameter uncertainty analysis

	Variance (%)	St. Deviation	Total Effect
Daily Evapotranspiration	0.01	0.01	0.01
Maximum Temperature	0.45	0.02	0.54
Minimum Temperature	0.18	0.01	0.32
Mean Temperature	2.07	0.04	2.39
Wind Speed	0.01	0.01	0.03
Relative Humidity	79.04	0.11	80.23
Solar Radiation	16.99	0.13	17.8

In the following table, parameters variances estimated to be deterministically sensitive at the Crop Water Shortage Index (23.8%), the second in order sensitive vegetation index is Water Supply Vegetation Index (22.9%), followed by Drought Severity Index (21.5%). The sum of the above three vegetation indices total effect is exceeding the value of 70% which implies the presence of interactions in term of dependency on the rest vegetation indices [41]. The least sensitive vegetation index is Daily Evapotranspiration (9.8%). Daily Evapotranspiration has the smallest individual contribution to the total variances [22,42].

According to figure 13, both of relative humidity and solar radiation considered to be the driving force of the uncertainty values of using SEBS model [41]. On the contrary, estimated daily evapotranspiration and wind speed variances are the least interconnected with the model uncertainty [43].

CONCLUSIONS

Simulated evapotranspiration through SEBS model demonstrated very high correlation with the ground truth data. Larger areas may be reliably assessed using space-borne data instead of in situ measurements. The application of the SEBS model over the entire study area mapped the daily evapotranspiration to be at maximum values of specific areas, within but mainly surrounding the Delta region. This fact may draw the attention of the decision makers towards adjustment of the agriculture practices in those areas and may propose proper land use changes. The study clearly brought out the spatial distribution of daily evapotranspiration derived from Remote Sensing data in conjunction with evaluation of biophysical variables of soil and topographic information in GIS context is helpful in crop management options for intensification or diversification.

Global Sensitivity Analysis of seven different metrological aspects delivered a quantitative and model independent sensitivity measures of each of the input factors and of groups of them to the simulated outputs under consideration. Results evidenced the model concept to be sufficiently sensitive to represent the natural systems' behavior. The sensitivity analysis confirmed that Daily Evapotranspiration is consecutively less sensitive among the different climatic input parameter based on water management hypothesis.

Input parameters are related directly to the estimated variables derived from the uncertainty analysis [41]. The global sensitivity analysis is used to identify the portions of the variance related to different measured input quantities. This method for sensitivity analysis is independent of the characteristics of the analyzed model.

This study has been done to find out the common thread in SEBS input parameter interconnections to achieve greater accuracy from remotely sensed data. Therefore, it gives primary results but for further study, additional factors like soil, irrigation facilities and socio-economic factors which influence the sustainable use of the land are required.

REFERENCES

1. Muthuwatta, L.P., M.D. Ahmad, M.G. Bos and T.H.M. Rientjes, 2010. Assessment of water availability and consumption in the Karkheh River Basin, Iran- using remote sensing and geo-statistics. *Water Resource Management*, 24: 459-484.
2. Sellers, P., D. Randall, J. Collatz, J. Berry, C. Field, D. Dazlich, C. Zhang, G. Collelo and A. Bounous, 1996. A revised land surface parameterization (SiB2) for atmospheric GCMs: Model formulation. *Journal of Climate*, 9: 676-705.
3. Su, W., T.P. Charlock and F.G. Rose, 2005. Deriving surface ultraviolet radiation from CERES surface and atmospheric radiation budget: Methodology, *Journal of Geophysical Research*, 110, D14209.
4. Allan, R.P., 2011. Combining satellite data and models to estimate cloud radiative effect at the surface and in the atmosphere. *Meteorological Applications*, 18: 324-333.
5. Allen, R., M. Tasumi and R. Trezza, 2007. Satellite-based energy balance for mapping evapotranspiration with internalized calibration (METRIC): Model ASCE. *Journal of Irrigation and Drainage Engineering*, 133(4): 380-394.

6. Chowdary, V.M., Y.K. Srivastava, V. Chandran and A. Jeyaram, 2009. Integrated water resource development plan for sustainable management of Mayurakshi watershed, India using remote sensing and GIS. *Water Resource Management*, 23: 1581-1602.
7. Kustas, W. and J. Norman, 1996. Use of remote sensing for evapotranspiration monitoring over land surfaces. *Hydrological Sciences Journal*, 41(4): 495-516.
8. Su, Z., M. Pelgrum and M. Menenti, 1999. Aggregation effects of surface heterogeneity in land surface processes. *Hydrology and Earth System Sciences*, 3(4): 549-563.
9. Jacob, F., A. Olioso, X. Gu, Z. Su and B. Seguin, 2002. Mapping surface fluxes using airborne visible, near infrared, thermal infrared remote sensing data and a spatialized surface energy balance model. *Agronomie*, 22: 669-680.
10. Kalma, J. and D. Jupp, 1990. Estimating evaporation from pasture using infrared thermometry: evaluation of a one-layer resistance model. *Agricultural and Forest Meteorology*, 51: 223-246.
11. Moran, M., T. Clarke, Y. Inoue and A. Vidal, 1994. Estimating crop water deficit using the relation between surface-air temperature and spectral vegetation index. *Remote Sensing of Environment*, 49: 246-263.
12. Olioso, A., H. Chauki, D. Courault and J. Wigneron, 1999. Estimation of evapotranspiration and photosynthesis by assimilation of remote sensing data into SVAT models. *Remote Sensing of Environment*, 68: 341-356.
13. Boegh, E., H. Soegaard and A. Thomsen, 2002. Evaluating evapotranspiration rates and surface conditions using Landsat TM to estimate atmospheric resistance and surface resistance. *Remote Sensing of Environment*, 79: 329-343.
14. Lagouarde, J., F. Jacob, X. Gu, A. Olioso, J. Bonnefond, Y. Kerr, K. McAneney and M. Irvine, 2002. Spatialization of sensible heat flux over a heterogeneous landscape. *Agronomie*, 22: 627-633.
15. Wu, C.D., H.C. Lo, C.C. Cheng and Y.K. Chen, 2010. Application of SEBAL and Markov models for future stream flow simulation through remote sensing. *Water Resource Management*, 24: 3773-3797.
16. Su, Z., 2001. A surface energy balance system (SEBS) for estimation of turbulent heat fluxes from point to continental scale. In: Su, Z., Jacobs, C. (Eds.), *Advanced Earth Observation Land Surface Climate*. Publications of the National Remote Sensing Board (BCRS), USP-2, 01-02, 184-185.
17. Su, Z., 2002. The surface energy balance system SEBS for estimation of turbulent heat fluxes. *Hydrology and Earth System Sciences*, 6(1): 85-99.
18. Su, Z., T. Schmugge, P. Kustas and J. Massman, 2001. An evaluation of two models for estimation of the roughness height for heat transfer between the land surface and the atmosphere. *Journal of Applied Meteorology*, 40(11): 1933-1951.
19. Petropoulos, G., M.J. Wooster, T.N. Carlson, M.C. Kennedy, and M. Scholze, 2009. A global Bayesian sensitivity analysis of the 1d SimSphere soil-vegetation-atmospheric transfer (SVAT) model using Gaussian model emulation. *Ecological Modelling*, 220: 2427-2440.
20. Saltelli, A., K. Chan and E.M. Scott, 2000. Sensitivity analysis. In: *Wiley series in probability and statistics* (pp: 467). Chichester: Wiley. ISBN:0-471-99892-3.
21. Saltelli, A., S. Tarantola, F. Campolongo and M. Ratto, 2004. Sensitivity analysis in practice: A guide to assessing scientific models (pp: 217). UK: Wiley. ISBN:0-470-87093-1.
22. Saltelli, A., 2002. Sensitivity analysis for importance assessment. *Risk Analysis*, 22(3): 549-590.
23. Saltelli, A., S. Tarantola and K.P.S. Chan, 1999. A quantitative model-independent method for global sensitivity analysis of model output. *Technometrics*, 41(1): 39-56.
24. Schwiager, V., 2004. Variance-based sensitivity analysis for model evaluation in engineering surveys. In *INGEO 2004 and FIG regional central and eastern European conference on engineering surveying Bratislava, Slovakia, November 11-13, 2004*.
25. Afify, A.A., S.M. Arafat and M.N. Aboel Ghar, 2011. Delineating rice belt cultivation in the Nile pro-delta of Vertisols using remote sensing data of Egypt Sat-1. *Journal of Agricultural Research*, 35(6): 2263-2279.
26. Elhag, M., A. Psilovikos and M. Sakellariou, 2013. Land use changes and its impacts on water resources in Nile Delta region using remote sensing techniques. *Environment, Development and Sustainability*, 15: 1189-1204.
27. Elhag, M., A. Psilovikos, I. Manakos and K. Perakis, 2011. Application of SEBS model in estimating daily evapotranspiration and evaporative fraction from remote sensing data over Nile Delta. *Water Resources Management*, 25(11): 2731-2742.
28. Huot, P., H. Tait, M. Rast, S. Delwart, L. Bézy and G. Levrini, 2001. The optical imaging instruments and their applications: AATSR and MERIS. *European Space Agency Bulletin*, 106: 55-66.

29. Menenti, M., 1984. Physical aspects and determination of evaporation in deserts applying remote sensing techniques Report 10 (Special issue). Institute for Land and Water Management Research (ICW). The Netherlands, pp: 202-203.
30. Su, Z., A. Yacob, J. Wen, G. Roerink, Y. He, B. Gao, H. Boogaard and C. Diepen, 2003. Assessing relative soil moisture with remote sensing data: theory, experimental validation and application to drought monitoring over the North China Plain. *Physics and Chemistry of the Earth*, 28: 89-101.
31. Su, W., A. Bodas-Salcedo, K.M. Xu and T.P. Charlock, 2010. Comparison of the tropical radiative flux and cloud radiative effect profiles in a climate model with Clouds and the Earth's Radiant Energy System (CERES) data. *Journal of Geophysical Research*, 115: D01105.
32. Liu, C. and H. Wang, 1999. The interface processes of water movement in the soil-crop-atmosphere system and water-saving regulation. Beijing Science Press, pp: 24-101.
33. Psilovikos, A. and M. Elhag, 2013. Forecasting of Remotely Sensed Daily Evapotranspiration Data over Nile Delta Region, Egypt, *Water Resources Management*, 27(12): 4115-4130.
34. Li, F., W. Kustas, J. Preuger, C. Neale and T. Jackson, 2005. Utility of remote sensing-based two-source balance model under low- and high-vegetation cover conditions. *Journal of Hydrometeorology*, 6: 878-891.
35. Li, Z., R. Tang, Z. Wan, Y. Bi, C. Zhou, B. Tang, G. Yan, and X. Zhang, 2009. A review of current methodologies for regional evapotranspiration estimation from remotely sensed data. *Sensors*, pp: 3801-3853.
36. Gontia, N.K. and K.N. Tiwari, 2010. Estimation of crop coefficient and evapotranspiration of wheat (*Triticum aestivum*) in an irrigation command using remote sensing and GIS. *Water Resource Management*, 24: 1399-14141.
37. Moran, M.S., A.F. Rahman, J.C. Washburne, D.C. Goodrich, M.A. Weltz and W.P. Kustas, 1996. Combining the Penman-Monteith equation with measurements of surface temperature and reflectance to estimate evaporation rates of semiarid grassland. *Agricultural and Forest Meteorology*, 80: 87-109.
38. Frey, C., G. Rigo and E. Parlow, 2007. Urban radiation balance of two coastal cities in a hot and dry environment. *International Journal of Remote Sensing*, 28(12): 2695-2712.
39. Elhag, M., 2014b. Sensitivity Analysis Assessment of Remotely Based Vegetation Indices to Improve Water Resources Management. *Environment Development and Sustainability*, DOI:10.1007/s10668-014-9522-0.
40. Frey, C., E. Parlow, R. Vogt, M. Harhash and M. Abel Wahab, 2010. Flux measurements in Cairo. Part 1: in situ measurements and their applicability for comparison with satellite data. *International Journal of Climatology*, Online early view.
41. Holvoet, K., A. van Griensven, P. Seuntjents and P.A. Vanrolleghem, 2005. Sensitivity analysis for hydrology and pesticide supply towards the river in SWAT. *Physics and Chemistry of the Earth*, 30: 518-526.
42. Giardino, C., M. Bresciani, P. Villa and A. Martinelli, 2010. Application of remote sensing in water resource management: The case study of Lake Trasimeno, Italy. *Water Resource Management*, 24: 3885-3899.
43. Jin, X., L. Wan and Z. Su, 2005. Research on evaporation of Taiyuan basin area by using remote sensing. *Hydrology and Earth System Sciences Discussion*, 2: 209-227.